VII International Conference on Particle-Based Methods
PARTICLES 2021
P. Wriggers, M. Bischoff, E. Oñate, A. Düster & T. Zohdi (Eds)

CFD-DEM SIMULATIONS OF THE BLAST FURNACE RACEWAY

FRANCIS ROMANO*†, EDOUARD IZARD* and PASCAL FEDE†

* ArcelorMittal Global R&D Maizières
Voie Romaine, 57280 Maizières-lès-Metz, France
e-mail: francis.romano@arcelormittal.com
e-mail: edouard.izard@arcelormittal.com

† Institut de Mécanique des Fluides de Toulouse (IMFT), Université de Toulouse, CNRS
Allée Prof. Camille Soula, 31400 Toulouse, France
e-mail: pascal.fede@imft.fr

Key words: Blast furnace, Raceway, CFD, DEM

Abstract. Gas injections at the bottom of the blast furnace create void regions in the coke matrix called the raceways which play a role in the gas distribution in the furnace and is directly linked to the iron production. In this region, complex physical phenomena occur, including particle-fluid interactions, and, as far as we know, there is no consensus on its shape and dynamics as well as its creation and stability. A better understanding of the raceway region could lead to a more efficient and stable blast furnace process. In order to clarify the main phenomena occurring in the raceway dynamics, we develop an unresolved CFD-DEM model of a 1/5 scale 2D slot pilot of the blast furnace for which typical experimental results are the monitoring of alternative raceway collapses. The CFD-DEM approach used solves the gas-solid flows where coke particles are modelled as a discrete phase and the gas as continuous using a RANS model. First, DEM simulations of the pilot are performed without the fluid contribution and show that its geometry influences the mechanical load applied on the raceway with a saturation of the granular stress inside the pilot. The Janssen model provides a good description of the measured load in the simulation. Then, the CFD-DEM model of the pilot permits to investigate the gas and granular flows when the raceway is imposed as in the experiment. The dynamics of the collapse with the coupling is simulated and displays a complex particle-gas 3d flow in which the cavity cannot stand as in the reference experiment. Finally, the CFD-DEM model provided with a simple cohesion model was able to reproduce the stability of the experimental cavity. This new cohesion mechanism plays a key role in the stability and, to our knowledge, for the first time identified.

1 INTRODUCTION

A blast furnace is a hot counter-current packed bed gas-solid-liquid reactor used in iron-making industry to produce steel where coke and iron bearing materials are alternatively charged in layers at the top of the furnace travelling downward in a quasi-static regime while a reducing hot gas injected at the bottom raceways ascends. Numerous physical processes are involved such as heat transfer, thermodynamics, chemical reaction and fluid-solid transport. In the bottom part of the blast furnace, hot air is injected laterally from tuyeres and create a void

region called raceway or cavity where heat and reducing gases are generated for the combustion of the material. The raceway plays a critical role in the gas distribution in the furnace and is directly linked to the iron production [1].

The access to measurements in the cavity being very challenging due to the extreme temperature and pressure conditions in these raceway zones, several researchers have set up laboratory experiments in order to better understand the phenomena of formation and fluctuation of the raceway [2], as we will detail in the section 2 of the paper. The experiments carried out at different scales on the formation and evolution of the cavity are essential to identify the main physical phenomena involved but do not provide a complete picture of the physical mechanisms. Therefore, together with the experiments, several researchers proposed different simulation methods with different scales of resolution in order to complete the observations. The continuum-based approach (Two-Fluid Model or TFM) and the discrete-based approach (CFD-DEM) are the most commonly used. In the TFM, both fluid phase and solid phase are treated as continuous media and described by Navier-Stokes equations [3]. For computational resources reasons, the TFM is more suitable for simulating large-scale systems. This aspect is important in the study of blast furnace cavities, particularly when trying to simulate the behavior of a full-size blast furnace. However, the understanding of some microscopic phenomena, such as the particle size distribution and the stresses in and around the cavity, is limited in this model. Such difficulties can be overcome by using the CFD-DEM model which describes each particle by Newton's equations, while the fluid is modeled by a continuous phase described by Navier-Stokes equations averaged within a computational cell where fluid-particle interactions are considered [4].

The article is structured as follows: First, the experimental raceway pilot and results are detailed. In a second step, the DEM and CFD-DEM used in this work and the careful choice of simulation parameters are presented. The static state of the pilot raceway is then studied with DEM simulations which show interesting constraints behaviours due to the discrete nature of the material. Finally, CFD-DEM simulations of the pilot are realized and permit to characterize the raceway collapse. The addition of a cohesion model shows to reproduce the experimental raceway stability and qualitative collapse behaviour.

2 DESCRIPTION OF THE PILOT AND EXPERIMENTAL RESULTS

The raceway pilot, as seen in the **Figure 1**, has been developed to study the influence of the process parameters on the raceway dynamics [8]. This model is designed to allow the observation of a raceway with combusting bed through a large window. The pilot is 1/5 scale size of typical blast furnace size which should respect the equilibrium constraints such as blast momentum and burning material column weight. This result to a pseudo two-dimensional model with a rectangular section of 830 mm long, 100 mm wide and 2.6 m high loaded with coke particles. Air at room temperature is brought to the model through a rectangular nozzle across the width of the model in order to respect 2D injection geometry as much as possible. The coke is ignited at the start of the test using a burner and combustion takes place with the cold air. A window allows to observe the temporal evolution of the cavity in front of the nozzle outlet. It is composed of double glazing made of quartz plate, reinforced by a metal mesh. A brick wall was built at the level of the air injection in order to respect the 10° angle formed by the blast furnace above the nozzle. A mesh hatch is placed under the coke bed, allowing only

ash and airflow to pass through a sealed ashtray. Air and combustion gases escape at the top through a chimney.

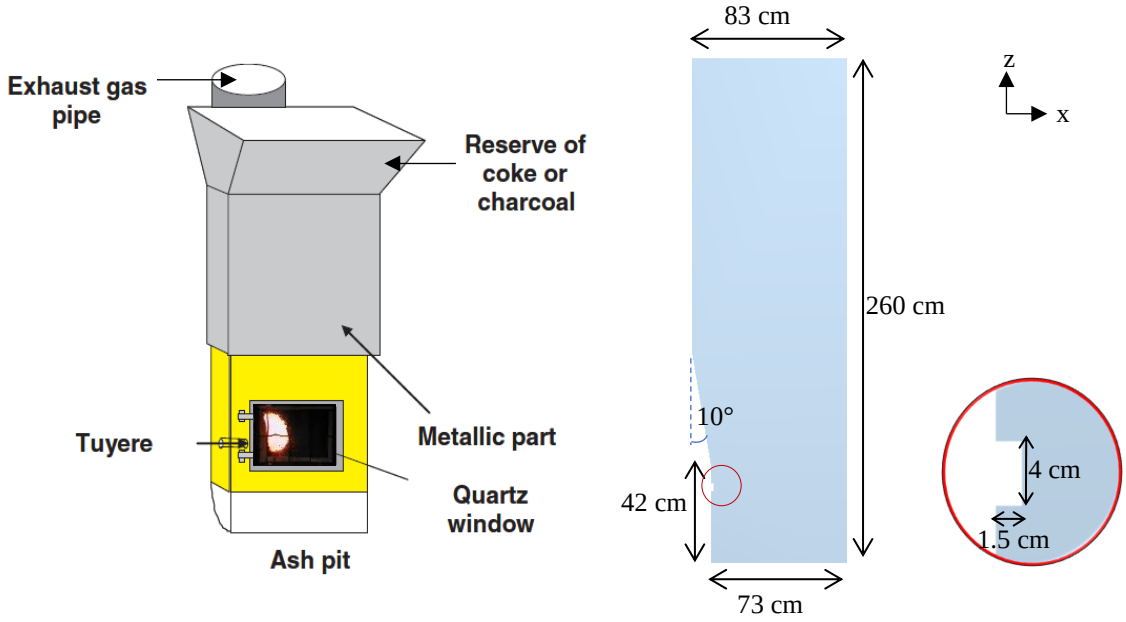

Figure 1: Schematic of the raceway pilot and geometry used for the simulation.

The main observation made with this hot model is that the cavity is not stable over long time, as seen in the **Figure 2**. It grows (Figure 2a) up to the arch formed over the cavity in the coke bed becomes unstable and collapses (Figure 2b). It is observed that the collapses occur mainly vertically (Figure 3c). Also, if one scrutinizes the images, one note that some particles stick to the refractory walls. The videos of the experiments show that some particles tend to agglomerate at the edge of the raceway. These observations have motivated subsequent numerical tests that we present in this paper.

(a) (b) (c)

Figure 2: Raceway collapsing during pilot operation from its maximal size (left image), during one collapse (in the center image) and after the collapse. For giving an idea of the collapse dynamics, the time from the left to the right images is aproximately 0.5s.

These experimental results will serve as reference data for comparisons to raceway simulations using CFD-DEM model that is presented in the next section.

3 MODEL DESCRIPTION

3.1 Particles flow model

All the particles considered in the simulations are spherical and polydisperse. The Discrete Element Method (DEM) used in the present work is based on the soft-particle approach developed by Cundall and Strack [10] and available in the commercial software EDEM (version 2019). In this method, the particles can slightly interpenetrate which allows the calculation of the contact forces from the history of these interpenetrations by a contact force model. One of the advantages of this method is to solve in dense and quasi-static particles flow with multiple inter-particle contacts which is of interest for understanding the formation and stability of the raceway. In DEM, the motion of each particle is determined by applying the fundamental principle of dynamics:

$$m_i \frac{d\boldsymbol{v}_i}{dt} = \sum_{j \neq i}^{N_p} \boldsymbol{F}_{c,j \to i} + \boldsymbol{F}_{pf,i} + m_i \boldsymbol{g} \tag{1}$$

$$I_i \frac{d\boldsymbol{w}_i}{dt} = \sum_{j \neq i}^{N_p} \boldsymbol{M}_{j \to i} \tag{2}$$

where N_p corresponds to the number of grains present in the simulation, m_i the mass of particle *i*, $\boldsymbol{v}_i$ its velocity and $\boldsymbol{F}_{pf,i}$ the particle-fluid interaction forces, $\boldsymbol{F}_{c,j \to i}$ the contact force of a particle *j* on a particle *i*, I_i its moment of inertia, $\boldsymbol{w}_i$ its rotation vector and $\boldsymbol{M}_{j \to i}$ the moment generated by the contact forces exerted by the particle *j* on the particle *i*. **g** is the gravity vector with a magnitude of $|\boldsymbol{g}| = 9.81 \text{m.s}^{-2}$ pointing the **-z** direction (see the **Figure 1** for the frame). Hertz-Mindlin model is used in this work to calculate the normal contact force [11]. The tangential contact force is based on the Mindlin-Deresiewicz work [12, 13]. Damping components are included in the normal and the tangential contact forces [14] and are related to the coefficient of restitution. The tangential contact force is bounded by the Coulomb law to model sliding, introducing the coefficient of static friction.

3.2 CFD-DEM solver

The modeling of the solid phase flow by DEM method is realized at the individual particle scale as described in the section 3.1, while that of the fluid phase flow is done by CFD. Fluid Mach number inside the raceway remaining below 0.3, therefore, the fluid is considered as incompressible. CFD-DEM simulations are isothermal where fluid density and viscosity correspond to air properties at 1600°C to simulate air flow at coke flame temperature. In the CFD-DEM approach, the fluid phase is described as a continuous medium based on the local resolution of the averaged Navier-Stokes equations. The equations governing the fluid flow are obtained by carrying out an averaging method locally as in the TFM method [17]. The governing equation for continuity (3) and momentum (4) in a computational cell are solved with the commercial software FLUENT (version 19.2) and can be written as follows:

$$\frac{\partial \Phi_f \rho_f}{\partial t} + \nabla \Phi_f \rho_f \boldsymbol{u}_f = 0 \tag{3}$$

$$\frac{\partial (\Phi_f \rho_f \boldsymbol{u}_f)}{\partial t} + \nabla (\Phi_f \rho_f \boldsymbol{u}_f \boldsymbol{u}_f) = -\Phi_f \nabla p + \nabla (\mu_f \Phi_f \nabla \boldsymbol{u}_f) + \Phi_f \rho_f \boldsymbol{g} - \boldsymbol{F}_{pf,i} \tag{4}$$

where Φ_f is the fluid volume fraction, ρ_f and μ_f are respectively the fluid density, $\boldsymbol{u}_f$ and p are the velocity and the pressure of the fluid, respectively. The particle-fluid interaction forces $\boldsymbol{F}_{pf,i}$ is the drag force exerted by the fluid on an individual particle i, of volume V_i, using the drag law proposed by Gobin et al. [18] which combines the equations of Wen & Yu [19] and Ergun [20]. Turbulence is modeled by using a standard k-ε model [21]. The fluid volume fraction, or porosity, Φ_f in each cell is obtained by the particle center method which consists of considering the total volume of the particle if its center is inside the cell:

$$\Phi_f = 1 - \frac{1}{\Delta V} \sum_{i=1}^{N_v} V_i \tag{5}$$

N_v being the number of particles in the fluid cell volume ΔV. The particle volume fraction inside a cell is defined by: $\Phi_p = 1 - \Phi_f$. The fluid time step is usually larger than the particle time step. At each fluid time step, the fluid solver calculates the velocity and pressure field of the fluid, as a function of particle data from the DEM model such as the solid volume fraction, thereby allowing the fluid drag forces to be calculated on each particle. These forces are then communicated to the DEM granular solver and make it possible to update the velocities and the positions of the particles up to the next fluid time step.

3.3 Simulation conditions

The computational domain used in DEM and CFD-DEM simulations is the same and correspond to the pilot's geometry. Several parameters were tested during pilot operation however we selected the maximal tuyere aperture (3mm), a bosh angle of 10°, no additional load over the coke bed and an air blast of 35 Nm^3/h. The granular phase, namely the coke, is represented by a log-normal distribution with a mean diameter of 5.5 mm and a span of 0.17. Particle size distribution is truncated at 3 mm as in the experiment. The Young's modulus of the particles in the simulation is relatively high to guarantee the hypothesis of non-deformable body right which ensures an accurate modelling of the contact between particles at high pressure [9]. The particle properties and DEM parameters employed in the simulation are given in **Table 1**. Coke particles are loaded from the top of the pilot and deposited under gravity until the pilot is full of 1,2 million of particles up to get a granular static state. The computational grids for the CFD has 14,868 cells of about 3 times a coke particle maximum diameter.

For the resolution of the fluid phase, 4 cores are used while the granular phase is solved using 8 cores with a graphic card unit which makes possible to considerably reduce simulation time for the DEM part. As an example, it takes 70 hours to simulate 0.2 seconds of physical flow.

Preliminary simulations will focus on the granular static state of the pilot by pure DEM simulations in which the granular stresses and particles properties are investigated. Then, CFD-DEM simulations are realized to model the fluid-particles flow inside the pilot.

Table 1: DEM parameters used in the simulations

Parameter	Value
Particle diameter min/max	3 mm/8 mm
Particle density	920 kg/m^3
Restitution coefficient	0.2
Particle/particle static friction	0.4
Particle/wall static friction	1
Rolling friction	0.01
Young's modulus	10^9 Pa
Poisson ratio	0.3
Particle time step	10^{-6} s
Fluid mass flow rate	0.013 kg/s
Fluid density	0.1885 kg/m^3
Fluid viscosity	5.457e-05 kg/m.s
Fluid time step	10^{-4} s

4 GRANULAR STATIC STATE

In this section, dry particles simulations are realized only with DEM activated in order to characterize the granular static state in the pilot.

4.1 Granular constraint and Janssen model

To measure the static state of the granular medium inside the pilot, the granular stress tensor in a defined control volume V is calculated as a function of velocity and force data from DEM as follows [15]:

$$\sigma_{ij} = -\frac{1}{V}\sum_{\alpha \epsilon V} m u_i'^{\alpha} u_j'^{\alpha} - \frac{1}{V}\sum_{c \epsilon V} f_i^c b_j^c \quad (6)$$

where u'^{α} is the velocity of the particle α, m its mass, f^c is the contact force between two particles at the contact, indexed with c, and b^c is the branch vector connecting the center of mass of the two particles in contact.

The vertical granular stress is investigated by creating 60 mm cube control volume containing around 1,360 particles. The pilot being 100 mm width, control volumes are placed at the center not to be influenced by the pilot transversal walls. Three profiles are then created at horizontal position $x = 175\ mm$, $x = 450\ mm$ and $x = 750\ mm$ by calculating the vertical component of the stress tensor σ_{zz} inside each control volume (**Figure 3**). The vertical granular stress at the top of the pilot follows the granulostatic pressure $\sigma_{zz} = \rho_p \Phi_p g z$ where ρ_p is the particle density, Φ_p the particle volume fraction, g the gravity acceleration and z the depth. The granulostatic pressure is linear and corresponds to the constraint at a certain depth of an unbounded domain. All three profiles show the similar trend: before a 0.3 m depth, granular pressure inside the pilot follows the granulostatic pressure and then saturates quickly after 0.5 m depth. This phenomenon is due to the redirection of the bed weight towards the pilot walls

by the formation of arches. The pilot being very narrow (about 20 coke particles across the width), the wall effect is even more important. This phenomenon is usually described by the Janssen model that evaluates the vertical mechanical stress σ_{zz} which saturates, as in grain silos [16], as a function of the geometry and particles properties.

$$\sigma_{zz} = \rho_p \Phi_p g \lambda (1 - e^{-\frac{z}{\lambda}}) \tag{7}$$

$$\lambda = \frac{L \times l}{2(L + l)\mu_w K} \tag{8}$$

L and l are the length and the width of the section, respectively, μ_w wall friction coefficient and $K = \sigma_{xx}/\sigma_{zz}=\sigma_{yy}/\sigma_{zz}$. The coefficient $K = 0.8$ has been extracted from the numerical simulation and averaged over the bed height.

Taking $\mu_w = 0.2$ the Janssen model is in good agreement with the simulation results as the granular pressure tends to a saturated value at the pilot bottom. For high depths $z \gg \lambda$, the granular stress tends towards $\rho_p \Phi_p g \lambda$. Note that this result is very difficult to measure in the experiment and is crucial to understand force balance on the particles occurring the pilot which shows the relevance of particle scale DEM simulations in the 2d raceway pilot.

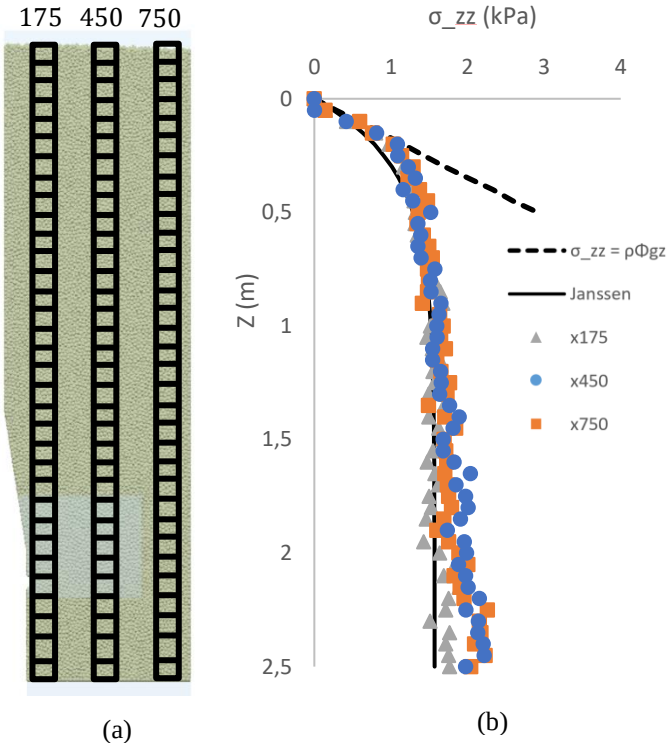

Figure 3: (a) Pilot filled with coke particles with the representation of the vertical control volume used for the stress measurements. (b) Vertical granular stress profiles at different pilot horizontal position x.

4.2 Effect of a prebuilt raceway on granular constraint

In this section, the simulation is carried with a prebuilt raceway which size and shape corresponds to the large size cavity measured in the pilot experiment. This raceway is obtained

by adding a wall representing the cavity as observed in experiments (**Figure 2**). The simulation is initialized in a similar manner than in the previous simulation with the same particle properties. The vertical profiles of vertical component of the granular stress are shown by **Figure 4**. The same tendency for granular pressure is obtained as expected: granulostatic evolution of the pressure at the top of the pilot and a saturation from a certain depth due to wall effect. The addition of a prebuilt cavity has affected the first two pressure profiles as they are close to the raceway region. Below the raceway, the granular stress has dropped and is evolving in a granulostatic manner with the increase of depth to reach again the saturated pressure. In a close region around the raceway, granular stress decreases a little as it can be observed on the $x = 175\ mm$ and $x = 450\ mm$ profiles from 1 m depth, the raceway furthest profile $x = 750\ mm$ remains constant.

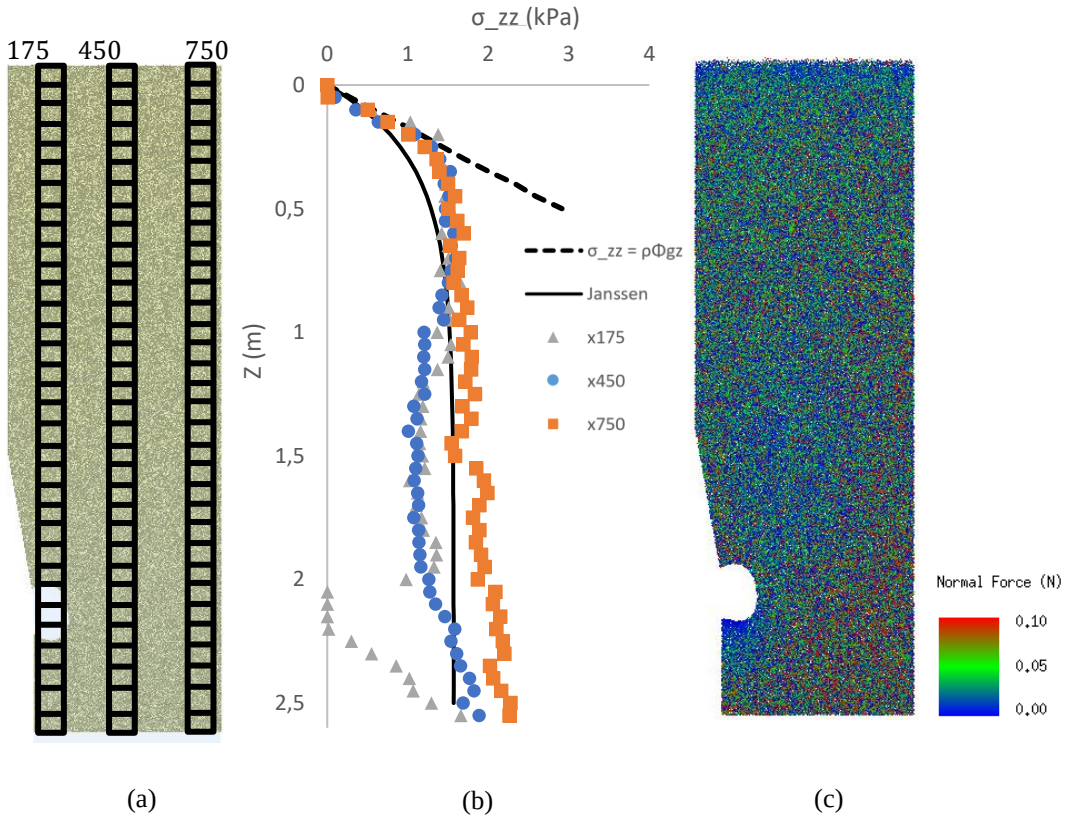

Figure 4: (a) Pilot with prebuilt raceway and vertical control volume for stress profiles. (b) Vertical granular stress profiles at different pilot location. (c) Particle-particle contact normal force inside the pilot.

5 RACEWAY COLLAPSING AND STABILITY

In this section, the CFD-DEM model, presented in the section 3, is used to investigate the particles-fluid flows when the cavity is imposed as in the experiments. The cavity wall is only seen by the particles in the simulation so that the fluid can flow through it. **Figure 5** shows the modulus of the gas velocity inside the cavity and the normalized gas velocity vector. Using air viscosity and density at 1600° lead to a 230 m/s velocity blast at the system inlet. Fluid velocity

drop quickly in the raceway as the pressure drop is large between the tuyere and the pilot outlet. The unsteady simulation is run until the gas dynamics reach a stable regime in time. The fluid enters inside the raceway in two directions: a counterclockwise direction over the tuyere and clockwise direction below. Particles-fluid interaction leads to a slightly decrease of the granular pressure at the interface between the raceway and the particles.

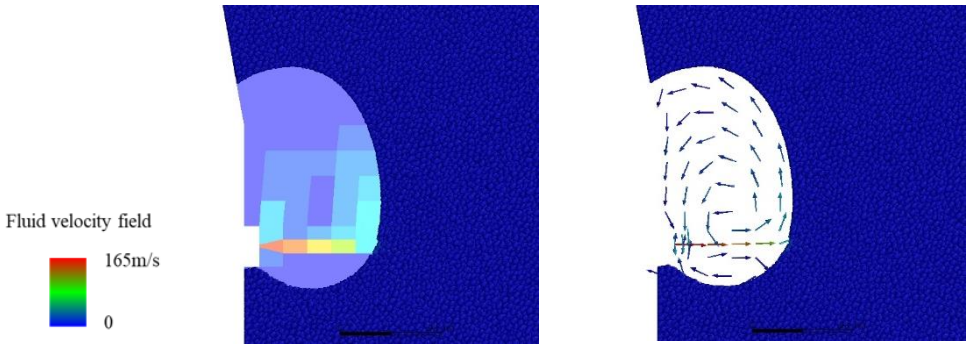

(a) (b)

Figure 5: (a) Fluid velocity field and (b) normalized velocity vectors inside the raceway for CFD/DEM simulation.

From the obtained stable regime of the system, the raceway wall that supports the granular material is removed from the simulation while fluid flow is still resolved. It is observed that the particles collapse by gravity. As soon as the raceway wall is removed, the granular column starts to fall as it can be seen by **Figure 6**. The drag and the friction forces are not sufficient for balancing the weight of the particle column. Over time a small cavity is formed with particles circulation clockwise and counterclockwise in front of the tuyere. These observations are in accordance with those of Cleary et al. [22].

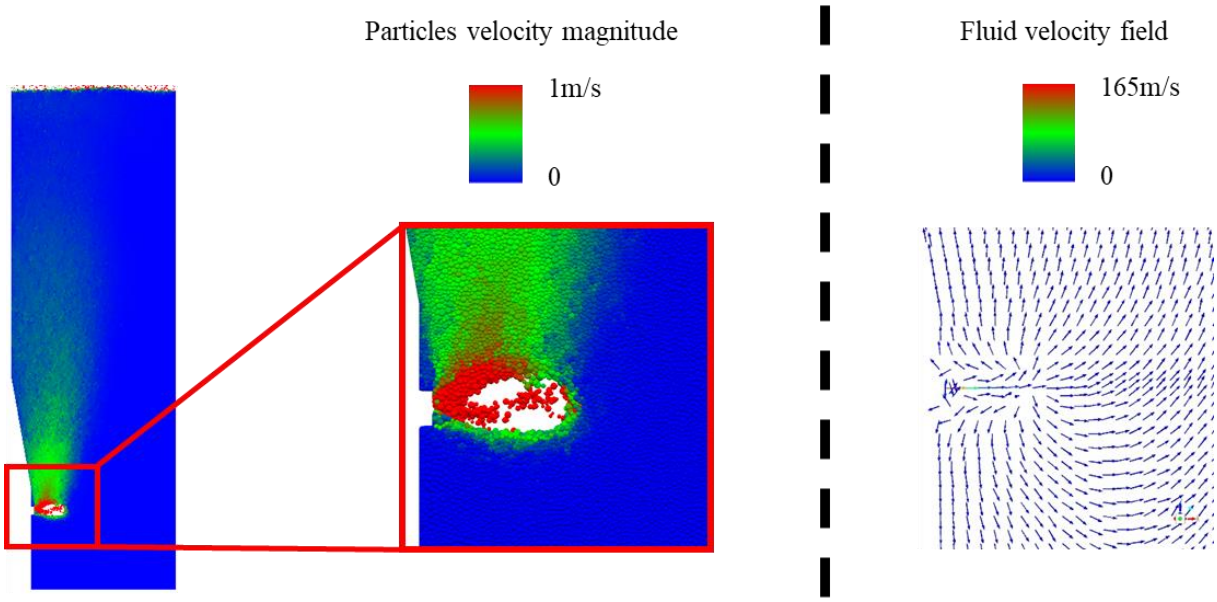

Figure 6: CFD-DEM simulation of raceway collapsing.

To obtain a stable raceway as in the experiments, we replace the Hertz-Mindlin contact model by the JKR cohesive contact model available in the EDEM software. JKR normal force is a function of the surface energy γ [23] which represents the magnitude of the cohesion forces embedded in a binary cohesive interaction. In the next numerical simulation, we consider larger coke particles using a log-normal distribution with a mean diameter of 10 mm and a span of 0.17.

The particle flow shows to be highly affected with the addition of this cohesion mechanism. Without the resolution of the fluid (DEM simulation only), for a given surface energy $\gamma = 10J/\mathrm{m}^2$ which indicates the cohesion intensity, the particles are stuck together and the raceway is maintained. At a lower magnitude cohesion energy $\gamma = 9J/\mathrm{m}^2$, the upper part of the cavity collapses vertically in a manner very close the observations in the experiments, as depicted the **Figure 7** which can be compared to **Figure 2**. The raceway collapsing time corresponds to the order of magnitude of a particle travel time in the raceway which means that the collapse dynamics is driven by gravity. Further numerical simulations (not shown) allows to understand that the greater the surface energy, the longer the collapse times. Also, using the same surface energy $\gamma = 9J/\mathrm{m}^2$ and activating the fluid flow resolution, CFD-DEM simulation results show that the raceway is now maintained (**Figure 8**). This means that together fluid drag force on particles and cohesion can overcome the granular column weight. In a similar manner that in the pilot experiment, it is observed that the formation of particles clusters at the raceway interface and crumbling of agglomerations due to competition between the cohesion and the weight of an agglomerate. These observations support the idea that there is a cohesive coke zone at the raceway interface.

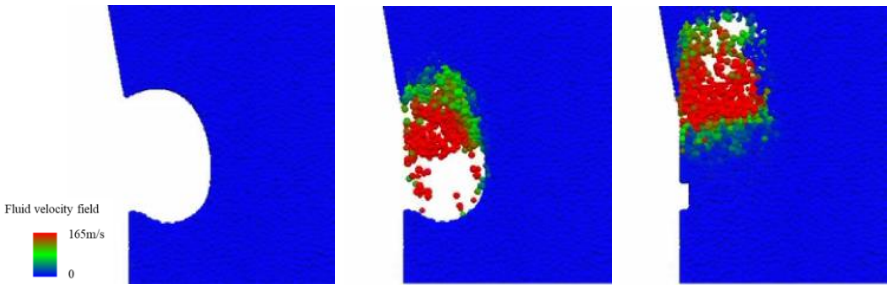

Figure 7: Temporal evolution of the raceway collapse simulation using the DEM simulation with the JKR contact model and a cohesion energy of $= 9J/\mathrm{m}2$.

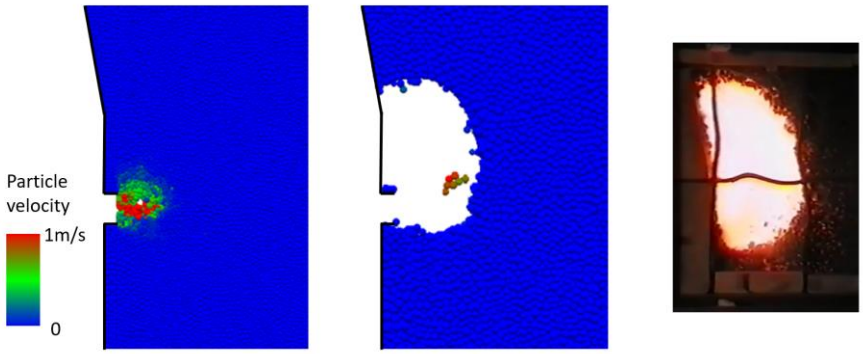

(a) (b) (c)

Figure 8: CFD/DEM simulation without (a) and with (b) cohesion. (c) Picture of the pilot experiment.

6 CONCLUSIONS

DEM and CFD-DEM simulations are carried out to improve the understanding of a hot raceway pilot by investigating the granular stress in the case of a prebuilt raceway. The conclusions from the present work is that granular pressure reaches a saturated value from a given depth due to the formation of arches which redirect the bed weight towards the pilot walls. Adding a prebuilt raceway tends to lower the pressure inside the pilot especially for vertical profile close to the raceway. Then, CFD-DEM model of the pilot permits to investigate the particles-fluid flows when the cavity is imposed as in the experiment. The dynamics of the collapse with the coupling shows an insufficient force balance to maintain the raceway. The CFD-DEM model provided with a JKR cohesion model was able to reproduce the stability and the collapse of the experimental cavity. Simulations results tend to show that a cohesive zone of coke exists at the raceway interface. Further implementation in the model will allow coke particle combustion and could permit to simulate the dynamics of the successive collapses as observed in the experiment. We are also interested to measure the properties of this particle scale hot cohesion mechanism we have identified and that plays a great role on the raceway stability at the pilot scale. Finally, our next objectives will be to develop more knowledge for full-scale blast furnace model perspectives; that is to perform accurate CFD-DEM simulations at the raceway blast furnace full-scale, as well as to provide coherent models to include in the TFM approaches.

7 REFERENCES

[1] Nishi, T., HARAGUCHI, H., MIURA, Y., SAKURAI, S., ONO, K., & KANOSHIMA, H. (1982). Relationship between Shape of Raceway and Productivity of Blast Furnace Taking Account of Properties of Coke Sampled at Tuyere Level. *Transactions of the Iron and Steel Institute of Japan*, *22*(4), 287-296.

[2] Flint, P. J., & Burgess, J. M. (1992). A fundamental study of raceway size in two dimensions. *Metallurgical and Materials Transactions* B, 23(3), 267-283.

[3] Mondal, S. S., Som, S. K., & Dash, S. K. (2005). Numerical predictions on the influences of the air blast velocity, initial bed porosity and bed height on the shape and size of raceway zone in a blast furnace. *Journal of Physics D: Applied Physics*, *38*(8), 1301.

[4] Zhu, H. P., Zhou, Z. Y., Yang, R. Y., & Yu, A. B. (2007). Discrete particle simulation of particulate systems: theoretical developments. *Chemical Engineering Science, 62*(13), 3378-3396.

[5] YUU, S., UMEKAGE, T., & MIYAHARA, T. (2005). Predicition of stable and unstable flows in blast furnace raceway using numerical simulation methods for gas and particles. *ISIJ international*, *45*(10), 1406-1415.

[6] Hager, Alice & Doppelhammer, Nikolaus & Kloss, Christoph & Pirker, Stefan. (2013). ON The formation of blast furnace raceways – A combines experimental and open source CFD-DEM. *Proc. Computational Modelling '13*.

[7] Miao, Z., Zhou, Z., Yu, A. B., & Shen, Y. (2017). CFD-DEM simulation of raceway formation in an ironmaking blast furnace. *Powder technology*, *314*, 542-549.

[8] Lectard, E., DANLOV, G., Blacknik, W., & MüLHEIMS, K. (2005). Optimisation of blast furnace raceway at high injection rates. EUR, (21691), 1-150.

[9] Agnolin, I., & Roux, J. N. (2007). Internal states of model isotropic granular packings. II. Compression and pressure cycles. *Physical Review E, 76*(6), 061303.

[10] Cundall, P. A., & Strack, O. D. (1979). A discrete numerical model for granular assemblies. *geotechnique, 29*(1), 47-65.

[11] Hertz, H. (1881). On the contact of elastic solids. *Z. Reine Angew. Mathematik*, *92*, 156-171.

[12] Mindlin, R. D. (1949). Elastic Spheres in Contact Under Varying Oblique Forces. *J. Applied Mechanics*, *16*(7), 327-330.

[13] Mindlin RD (1953) Elastic spheres in contact under varying oblique forces. *J. Applied Mech., 20*, 327-344

[14] Tsuji, Y., Tanaka, T., & Ishida, T. (1992). Lagrangian numerical simulation of plug flow of cohesionless particles in a horizontal pipe. *Powder technology*, *71*(3), 239-250.

[15] Goldenberg, C., Atman, A. P., Claudin, P., Combe, G., & Goldhirsch, I. (2006). Scale separation in granular packings: stress plateaus and fluctuations. *Physical review letters, 96*(16), 168001.

[16] Bruno, A., Forterre, Y., & Pouliquen, O. (2011). *Les milieux granulaires: entre fluide et solide*. Savoirs Actuels.

[17] Anderson, T. B., & Jackson, R. (1967). Fluid mechanical description of fluidized beds. Equations of motion. *Industrial & Engineering Chemistry Fundamentals, 6*(4), 527-539.

[18] Gobin, A., Neau, H., Simonin, O., Llinas, J. R., Reiling, V., & Sélo, J. L. (2003). Fluid dynamic numerical simulation of a gas phase polymerization reactor. *International journal for numerical methods in fluids*, 43(10-11), 1199-1220.

[19] Wen, C. Y. (1966). Mechanics of fluidization. In *Chem. Eng. Prog. Symp. Ser*. (Vol. 62, pp. 100-111).

[20] Ergun, S. (1952). Fluid flow through packed columns. *Chem. Eng. Prog.*, 48, 89-94

[21] Nallasamy, M. (1987). Turbulence models and their applications to the prediction of internal flows: a review. *Computers & Fluids, 15*(2), 151-194.

[22] Hilton, J. E., & Cleary, P. W. (2012). Raceway formation in laterally gas-driven particle beds. *Chemical engineering science*, *80*, 306-316.

[23] Johnson, K. L., Kendall, K., & Roberts, A. (1971). Surface energy and the contact of elastic solids. *Proceedings of the royal society of London. A. mathematical and physical sciences, 324*(1558), 301-313.